Supporting Information

Tailoring Interfacial Carrier Dynamics *via* Rationally Designed Uniform $CsPbBr_xI_{3-x}$ Quantum Dots for High-Efficiency Perovskite Solar Cells

Shuguang Zhang,[#ab] Young Jun Yoon,[#b] Xun Cui,[b] Yajing Chang,[b] Meng Zhang,[b] Shuang Liang,[b] Cheng-Hsin Lu,[b] and Zhiqun Lin[*b]

[a] *Department of Electronic Materials, School of Materials Science and Engineering, South China University of Technology, Guangzhou 510640, China.*

[b] *School of Materials Science and Engineering, Georgia Institute of Technology, Atlanta, Georgia 30332, USA.*

[#] *These authors contribute equally to this work*

**E-mail: zhiqun.lin@mse.gatech.edu*

Experimental Section

Materials:

Methylammonium iodide (CH_3NH_3I; MAI) were synthesized according to the previous method,[1] and dried in a vacuum oven at 50 °C for 24 hrs. *β*-Cyclodextrin (*β*-CD), *Tert*-Butyl acrylate (*t*BA, 98%), Titanium diisopropoxide bis(acetylacetonate) (Tiacac, 75 wt% in isopropanol), titanium (IV) chloride ($TiCl_4$, 99.995%), lead iodide (PbI_2, 99.999%), Dimethylformamide (DMF, anhydrous, 99.9%), Tetrahydrofuran (THF, 99%), *N, N, N′, N″, N″*-pentamethyldiethylene triamine (PMDETA, 99%), Trifluoroacetic acid (TFA, 99.9%) were purchased from Sigma Aldrich and used as reveiced. Lead bromide ($PbBr_2$, 99.995%) was purchased from TCl. Cesium bromide (CsBr, 99.999%) was purchased from STREM

Chemicals. Acetone (ACS reagent grade) and toluene (ACS reagent grade) were purchased from BDH Chemicals and used as received. CuBr (Sigma Aldrich, 98%) were purified via stirring overnight in acetic acid for 15 h, filtered, and washed subsequently with ethanol and diethyl ether completely, and dried under vacuum prior to use. *t*BA and styrene (St, Sigma-Aldrich, ≥99%) was washed with 10% NaOH aqueous solution and water successively, dried over calcium hydride (CaH_2), and distilled under reduced pressure. All other reagents were purified by common purification procedures.

Synthesis of Multi-arm Star-like Poly(tert-Butyl Acrylate) (Star-like PtBA)

Heptakis[2,3,6-tri-O-(2-bromo-2-methylpropionyl)]-β-cyclodextrin (21Br-β-CD) was synthesized according to a previously reported procedure.[1, 2] Star-like P*t*BA was synthesized through atom transfer radical polymerization (ATRP) of *t*BA monomers grafting from the 21Br-β-CD macroinitiator. Briefly, CuBr (35.0 mg), *N, N, N′, N″, N‴*-pentamethyldiethylene triamine (PMDETA, 85.0 mg), 21Br-β-CD (50 mg), tBA (21 mL), and 2-butanone (21 mL) were mixed in an ampoule. The ampoule bubbled with argon to remove oxygen and then tightly sealed before placing in an oil bath at 60 °C for desired reaction time. To terminate the reaction, the ampuole was quenched by cooling the ampoule in liquid nitrogen and exposing the solution to air. The solution was then diluted with THF or acetone and passed through an alumina column to remove the CuBr catalyst, followed by fractional precipitation with a volume ratio of methanol/water of 1/1 to remove monomers and linear P*t*BA. The product was then fully dried at 40 °C under vacuum before further processing.

Synthesis of Multi-arm Star-like Poly(tert-Butyl Acrylate)-block-Polystyrene (Star-like PtBA-b-PS)

Star-like P*t*BA-*b*-PS was synthesized via ATRP of styrene (St) monomers grafting from the star-like P*t*BA containing terminal –Br groups as the ATRP initiator (i.e., star-like P*t*BA-Br). Briefly, star-like P*t*BA-Br (i.e., Br in P*t*BA macroinitiator) : CuBr : PMDETA : styrene = 1 : 1 : 2 : 800 (molar ratio) in anisole (1ml solvent per 1g styrene) were mixed in an ampoule. After bubbling with argon, the ampoule was then tightly sealed and placed in an oil bath at

90 °C. After the desired reaction time, the reaction was quenched by cooling the ampoule in liquid nitrogen and exposing the solution to air. The product solution was diluted with THF or acetone and passed through an alumina column to remove the catalyst, and then subsequently purified by fractional precipitation with methanol/water as the precipitator to remove unreacted monomers and linear PS. The product was then dried at 40 °C under vacuum for at least 24 hr prior to use.

Synthesis of Multi-arm Star-like Poly(Acrylic Acid)-block-Polystyrene (PAA-b-PS) (Star-like PAA-b-PS)

Star-like PAA-*b*-PS was prepared by hydrolyzing the tert-butyl ester groups of P*t*BA blocks of star-like P*t*BA-*b*-PS to acrylic acid groups. Briefly, Star-like P*t*BA-*b*-PS was first completely dissolved in dichloromethane, followed by the slow addition of trifluoroacetic acid. The solution was left to react at room temperature for 24 hr. The solvent was then evaporated under reduced pressure at 30 °C. The final product was then washed with methanol, and fully dried under vacuum at 40 °C for at least 24 hrs.

Synthesis of PS-ligated $CsPbBr_3$ quantum dots (QDs)

PS-ligated $CsPbBr_3$ QDs were synthesized by utilizing star-like PAA-*b*-PS as nanoreactors. The percursors are selectively partitioned in the space occupied by the inner hydrophilic PAA blocks of star-like PAA-*b*-PS. The strong coordination interaction between perovskite precursors (CsBr and $PbBr_2$) and the carboxylic groups of inner PAA blocks of the nanoreactor facilitates the loading of precursors within the inner PAA compartment. Upon introducing precursors-loaded star-like PAA-*b*-PS into toluene (a non-solvent for $CsPbBr_3$), PS-ligated $CsPbBr_3$ QDs are instataneously formed. In a typical procedure, star-like PAA-*b*-PS nanoreactors, CsBr and $PbBr_2$ were dissolved in DMF at room temperature. In order for the precursors to preferentially siutatate within the inner PAA compartment of the nanoreactor, the solution was stirred for more than 24 hrs. The solution was then added into toluene, upon which $CsPbX_3$ QDs immediately formed in solution.

Synthesis of PS-ligated $CsPbBr_xI_{3-x}$ Quantum dots (QDs)

PS-ligated $CsPbBr_xI_{3-x}$ QDs were synthesized by anion exchange method, which has been reported in the literature. Briefly, after the synthesis of PS-capped $CsPbBr_3$ QDs, zinc iodide solution was firstly prepared by dissolving an appropriate amount of zinc iodide into methanol. The zinc iodide solution was then added in drops into a PS-ligated $CsPbBr_3$ QDs-containing vial during which virgorous strirring was on process. The Br/I ratio of $CsPbBr_xI_{3-x}$ QDs was judiciously tailored by virgorously adjusting the molar ratio of zinc iodide to that of PS-ligated $CsPbBr_3$ QDs.

Fabrication of Perovskite Solar Cells with and without PS-ligated $CsPbBr_xI_{3-x}$ Quantum Dots

Fluorine-doped tin oxide (FTO)-coated transparent glass substrates were etched with HCl (4 M) and metallic zinc powder, and sequentially ultrasonically cleaned using grease remover, DI water, acetone, n-butyl alcohol, and ethanol for 20 min, respectively. The clean FTO was then treated using oxygen plasma for 15 min, followed by spin-coating 0.15 M titanium diisopropozisw bis(acetylacetonate) solution at 3000 r.p.m for 30 s. The titanium-containing precusor film was placed on the hot plate at 125 ^oC for 10 min and then annealed in the furnace at 500 ^oC for 60 min. The resulting TiO_2 was then immersed into a 20-mM $TiCl_4$ solution at 70 ^oC for 40 min to generate a compact TiO_2 film. Then a layer of mesoporous TiO_2 was spun on top of the compact TiO_2 film at 3000 r.p.m for 30 s using TiO_2 paste, followed by a rapid annealing at 500 ^oC for 30 min. The $MAPbI_3$ layer was then spin-coated on mesoporous TiO_2 surface using the tranditional approach at 4500 r.p.m for 35s using diethyl ether as anti-solvent solution inside the glove box filled with Ar atmosphere. After diethyl ether-induced antisolvent process, all the samples were positioned on the surface of a hot plate at 100 ^oC for 15 min for further crystallization of $MAPbI_3$. The PS-ligated $CsPbBr_xI_{3-x}$ QDs of varied compositions and concentrations were then spin-coated on top of the $MAPbI_3$ film at 3000 rpm for 30 s, followed by a post-annealing process at 100 ^oC for 10 min. For the Spiro-OMeTAD hole-transport layer deposition, 72.3 mg Spiro-OMeTAD power was dissolved into 1 mL Chlorobenzene, mixed with 28.8 µl 4-tert-butylpyridine (TBP) and 17.5 µl Li-bis(trifluoromethanesulfonyl) imide (Li-TFSI) using acetonitrile as solvent (520 mg/ml). The resulting Spiro-OMeTAD solution was

spun on the PS-ligated $CsPbBr_xI_{3-x}$ QDs-deposited $MAPbI_3$ film at 3000 r.p.m for 30 s. Finally, Ag electrode of 150 nm was thermally evaporated. Control devices without the use of PS-ligated $CsPbBr_xI_{3-x}$ QDs to interface $MAPbI_3$ and Spiro-OMeTAD were also fabricated with the same preparative procedures for comparison.

Characterization

The number average molecular weight, M_n, and polydispersity index, PDI, were measured by gel permeation chromatography (GPC) equipped with an LC-20 AD HPLC pump and a refractive index detector (RID-10A, 120 V) at room temperature. All proton nuclear magnetic resonance (NMR) spectra of star-like P*t*BA and star-like P*t*BA-*b*-PS and star-like PAA-*b*-PS were presented using a Varian VXR-300 microscopy. The optical properties of $MAPbI_3$ film and PS-ligated $CsPbBr_xI_{3-x}$ QDs were characterized by UV-vis spectrophotometer (SHIMADZU, UV-2600) with Halogen lamp and Deuterium lamp as excitation sources. The crystal structures of $MAPbI_3$ with and without PS-ligated $CsPbBr_xI_{3-x}$ QDs decoration were characterized by the XRD (X'pert PRO, Netherlands) using Cu $K\alpha_1$ (λ=1.5401 Å) radiation. The scanning electron microscopy (SEM) images were obtained using Hitachi SU8000 equipped with high energy electron sources and stunningly sensitive detector system. The steady-state photoluminescence (PL) was collected using Spectrofluorometer (RF-5301PC, SHIMADZU). The time-resolved PL measurements were performed using a Photon Technology International (PTI) LaserStrobe Spectrofluorometer equipped with a PTI GL-3300 nanosecond nitrogen laser (λ=337 nm) and Photomultiplier tubes (PMT) together with time-correlated single photon counting (TCSPC) for single collection and analysis. For perovskite solar cells characterization, the current density-voltage (*J-V*) curves were measured using the Newport AM 1.5G solar simulator together with a Keithley 2601A multisource meter under ambient conditions. The *J-V* curves were scanned in both forward and reverse directions with varied scanning rate and time interval. The external quantum efficiency (EQE) measurement was performed using a Newport Quantum Efficiency Measurement Kit. Electrochemical Impedance spectroscopy was collected using the Zennium electrochemical workstation (Zahner). The controlled intensity modulated photovoltage spectroscopy (CIMVS) and controlled intensity modulated photocurrent spectroscopy (CIMPS) measurements were

carried out using the Zahner electrochemical workstation, together with PP211 power potentiostat and light source control module.

Figures and Tables

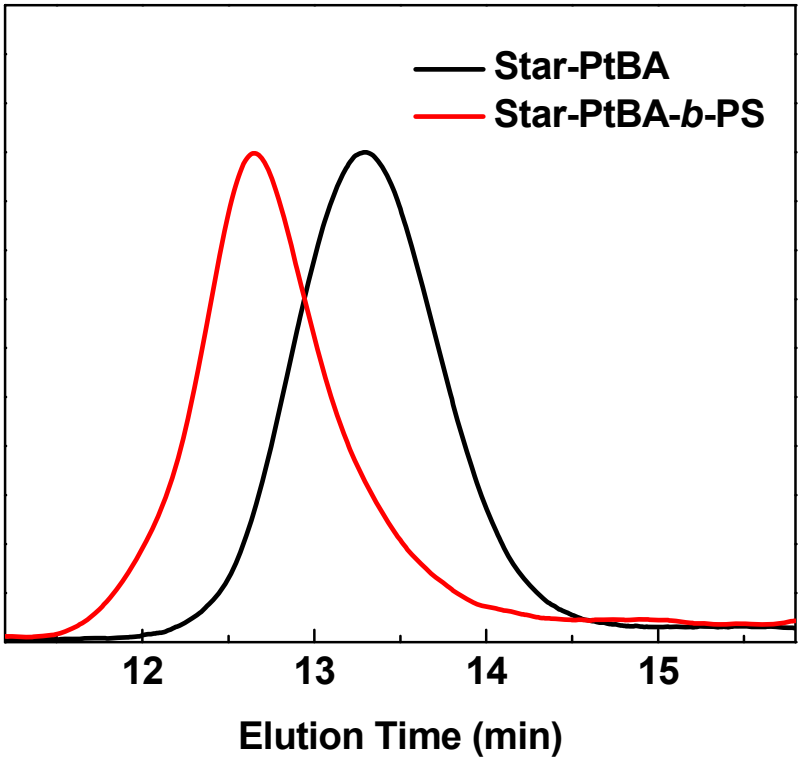

Figure S1. GPC traces of star-PtBA and star-PtBA-*b*-PS, respectively.

Table S1. Summary of molecular weights of amphiphilic star-like PAA-*b*-PS diblock copolymers.

Samples	M_n (kg/mol)	PDI	$M_{n,\,PAA}$ per arm (kg/mol) by ^{2}H-NMR	$M_{n,\,PS}$ per arm (kg/mol) by ^{3}H-NMR
Star-like PtBA	193	1.14	N/A	N/A
Star-like PAA-*b*-PS	307	1.22	11.0	7.7

Notes: M_n = number average molecular weight. *PDI* = polydispersity index.

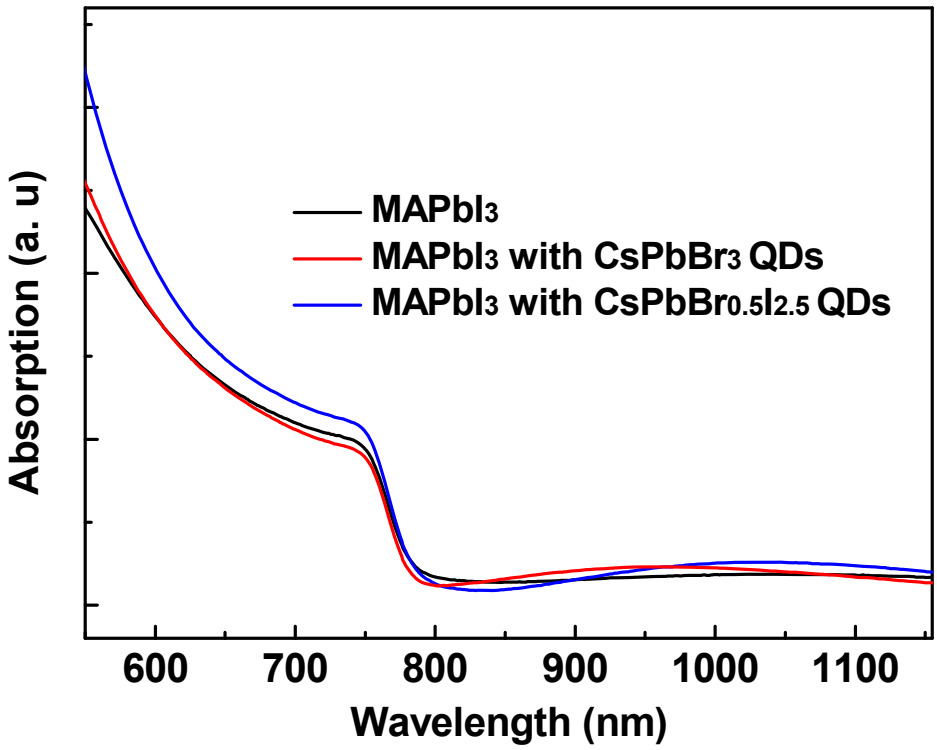

Figure S2. UV-vis absorption spectra of perovskite $MAPbI_3$ film with and without the PS-ligated -$CsPbX_3$ QDs modification, respectively.

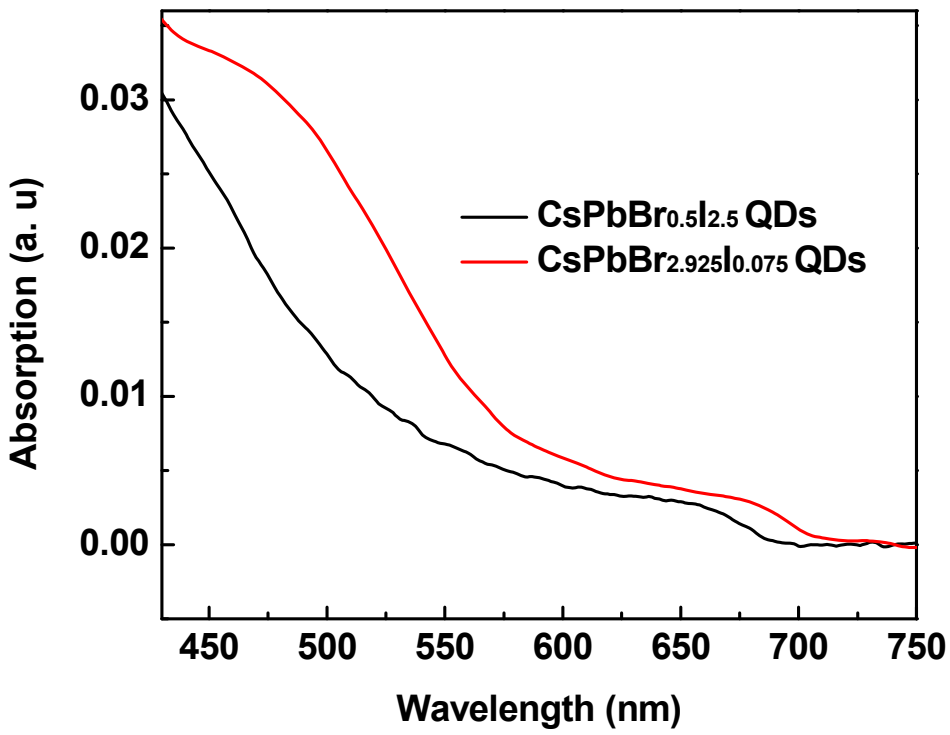

Figure S3. UV-Vis absorption spectra of PS-ligated $CsPbBr_{0.5}I_{2.5}$ and $CsPbBr_{0.075}I_{2.925}$ QDs, respectively.

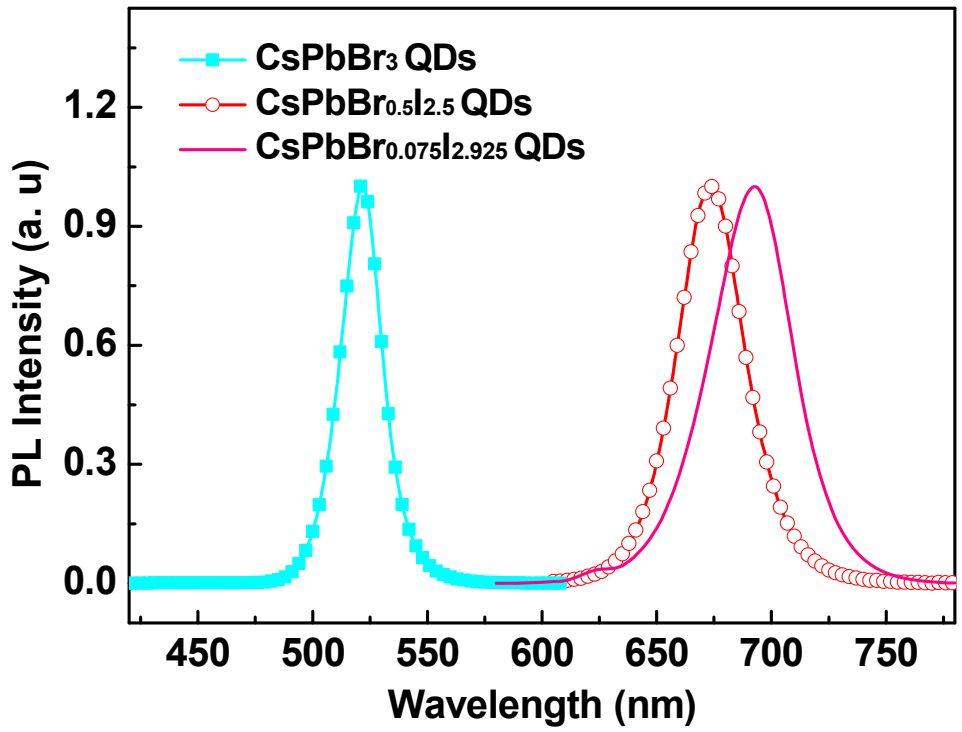

Figure S4. Normalized steady-state PL of PS-ligated $CsPbBr_3$, $CsPbBr_{0.5}I_{2.5}$, and $CsPbBr_{0.075}I_{2.925}$ QDs, respectively.

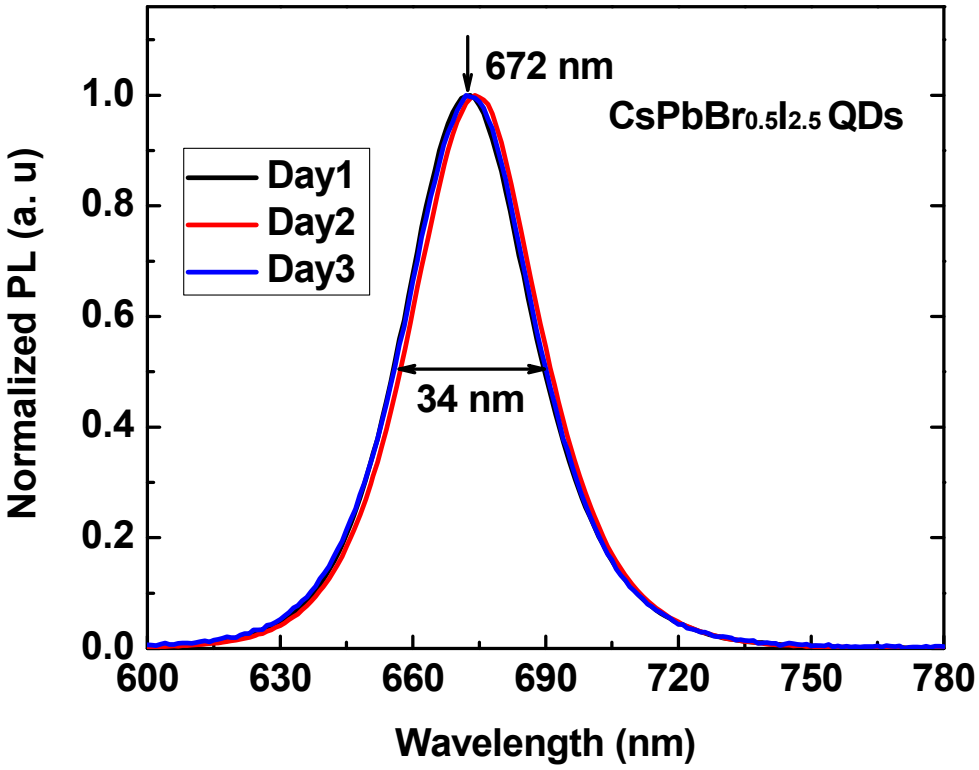

Figure S5. Normalized steady-state PL of PS-ligated $CsPbBr_{0.5}I_{2.5}$ QDs, synthesized by capitalizing on star-like PAA-*b*-PS diblock copolymer as nanoreactor, after 1 day, 2 days, and 3 days at room temperature, respectively. The PS-ligated $CsPbBr_{0.5}I_{2.5}$ QDs solution was stored under ambient condition, exposing to air (humidity ~30 %) and room light without stirring. The negligible peak shift is clearly evident, indicating outstanding colloidal stability of PS-ligated $CsPbBr_{0.5}I_{2.5}$ QDs.

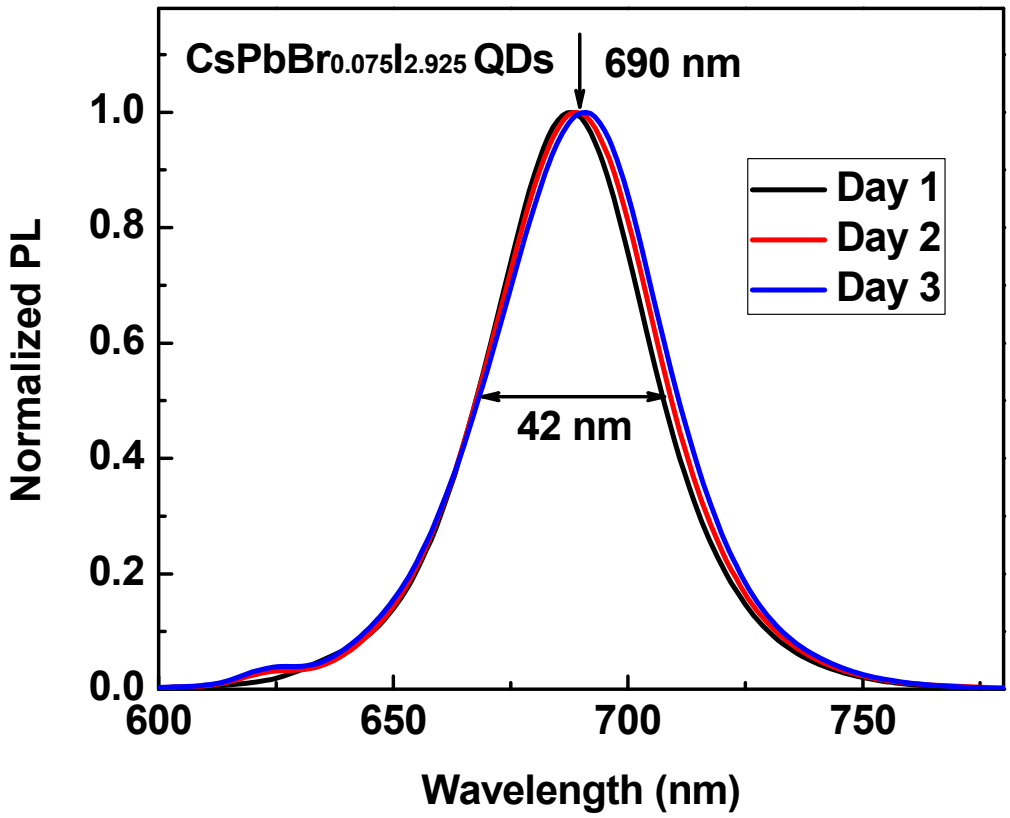

Figure S6. Normalized steady-state PL of PS-ligated $CsPbB_{0.075}I_{2.925}$ QDs, synthesized by capitalizing on star-like PAA-*b*-PS diblock copolymer as nanoreactor, after 1 day, 2 days, and 3 days at room temperature, respectively. The $CsPbB_{0.075}I_{2.925}$ QDs solution was stored under ambient condition, exposing to air (humidity ~30 %) and room light without stirring. Similar to PS-ligated $CsPbB_{0.5}I_{2.5}$ QDs, these QDs show excellent stability with the PL peak position centered around 690 nm.

Table S2. Summary of PL decay parameters obtained from a biexponential fitting of the time-resolved PL decay curves for $CsPbBr_3$ and $CsPbBr_{0.5}I_{2.5}$ QDs, respectively.

Sample	A_1	τ_1 (ns)	A_2	τ_2 (ns)	τ_{ave} (ns)
$CsPbBr_3$	0.562	39.49	0.066	204.00	101.60
$CsPbBr_{0.5}I_{2.5}$	0.496	25.45	0.335	128.86	145.46

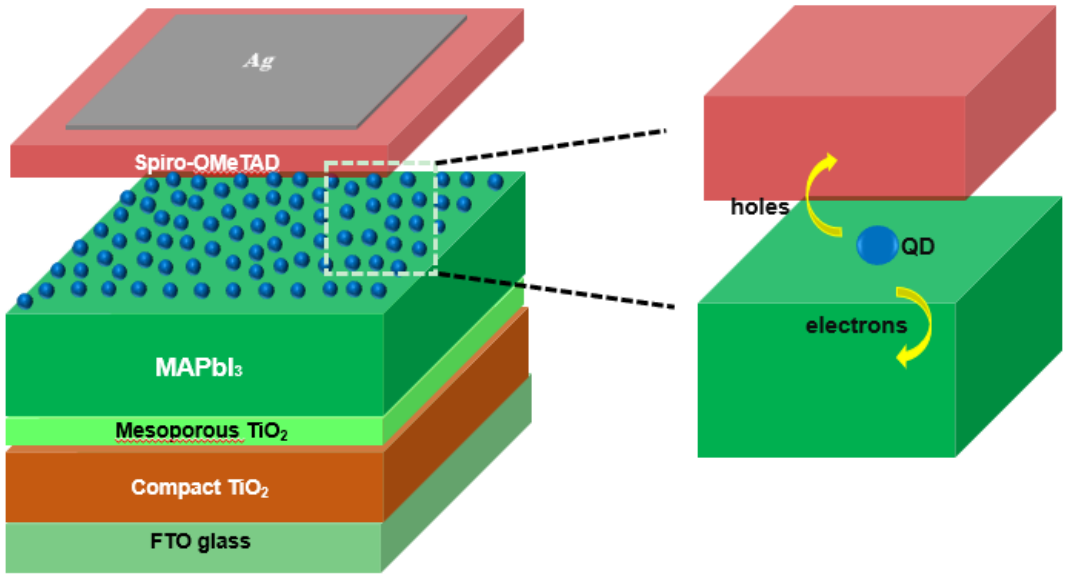

Figure S7. Schematic illustration of the device structure composed of $CsPbBr_{0.5}I_{2.5}$ QDs situated at the $MAPbI_3$/Spiro-OMeTAD interface.

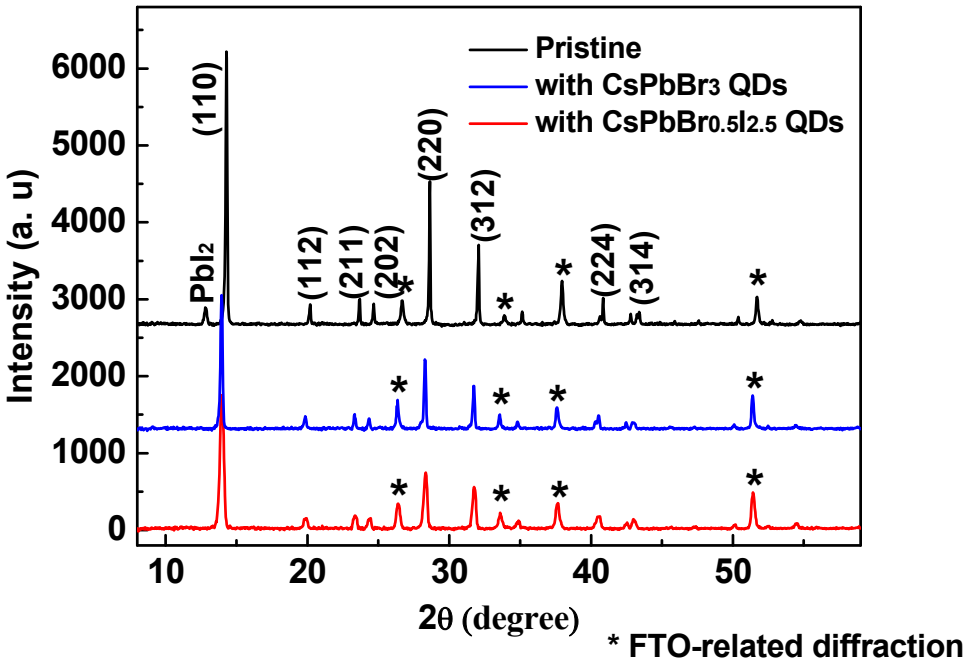

Figure S8. XRD profiles of $MAPbI_3$ film without and with the deposition of PS-ligated $CsPbBr_3$ and $CsPbBr_{0.5}I_{2.5}$ QDs on the surface. The small peak at 2θ of ~12.8° can be attributed to the PbI_2-related diffraction. No characteristic peaks of PS-ligated $CsPbBr_3$ and $CsPbBr_{0.5}I_{2.5}$ QDs can be seen owing to the inappreciable amount of QDs on the $MAPbI_3$ surface. Reduced intensity of $MAPbI_3$ with QDs can be ascribed to the QDs scattering-induced diffraction reduction.

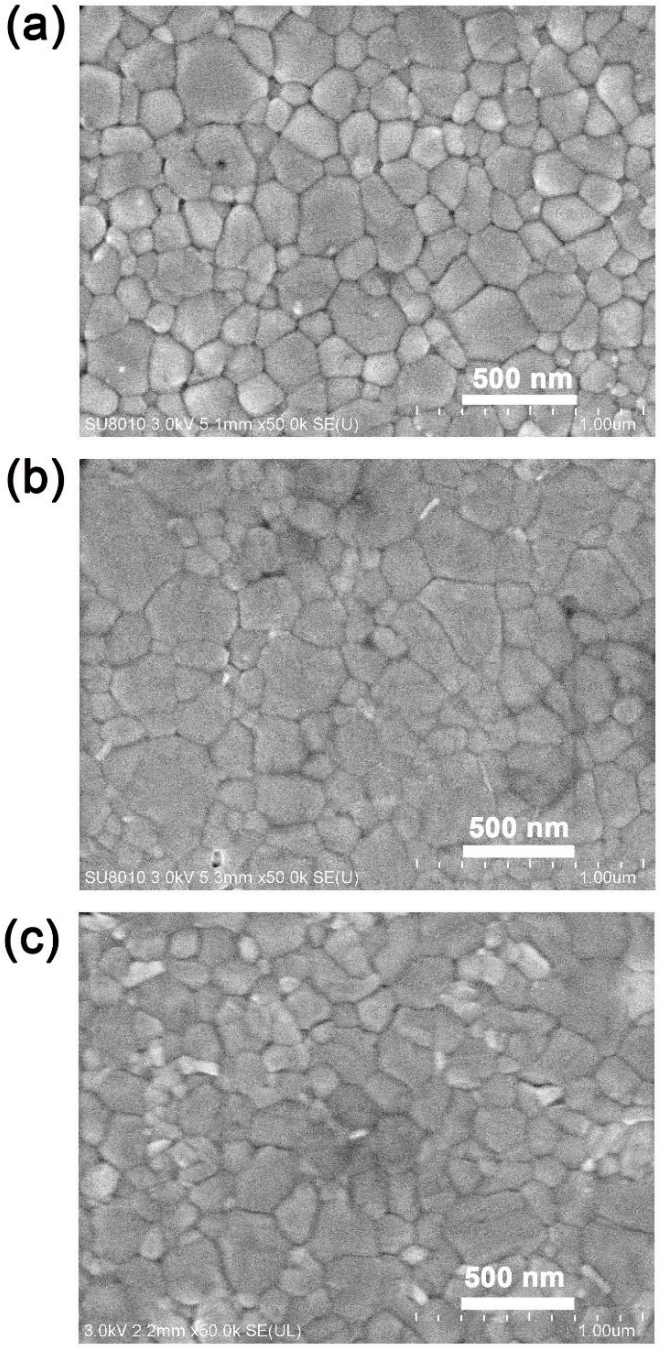

Figure S9. Top-view SEM images of (a) pristine $MAPbI_3$ film, and with (b) PS-ligated $CsPbBr_3$ and (c) PS-ligated $CsPbBr_{0.5}I_{2.5}$ QDs deposited on the surface.

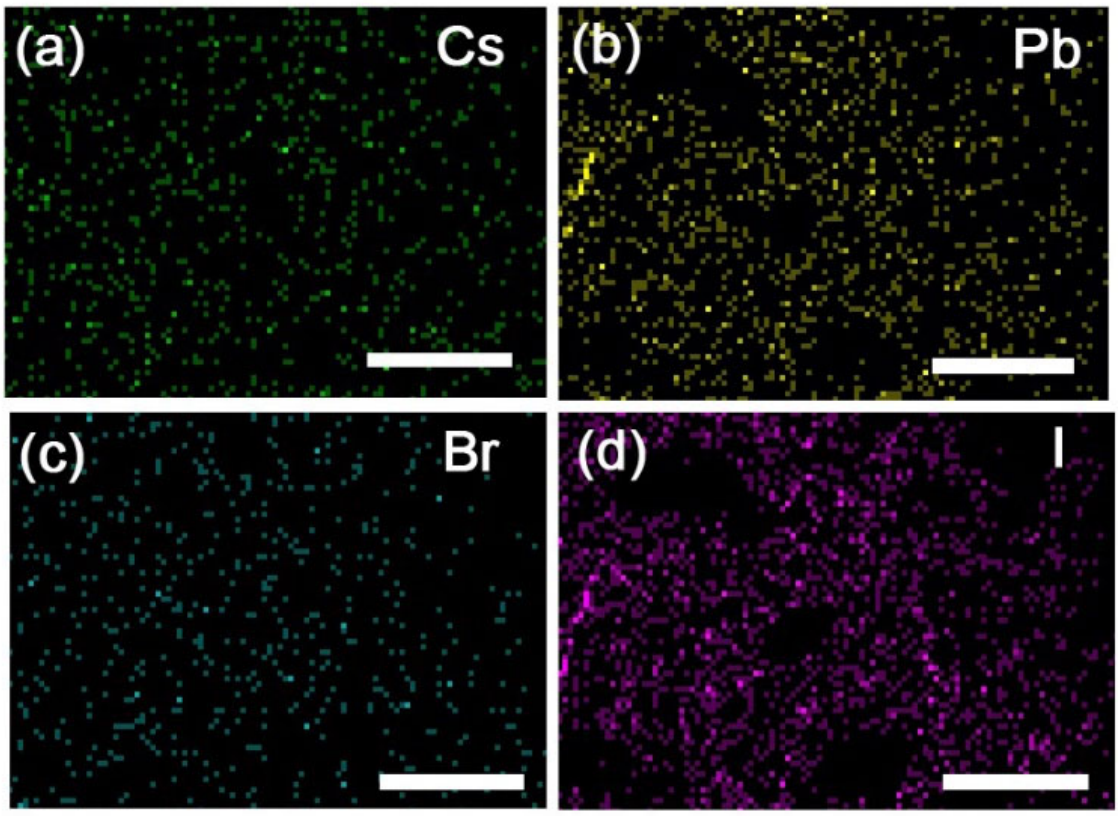

Figure S10. EDS mapping images of (a) Cs, (b) Pb, (c) Br and (d) I from the $MAPbI_3$ film with PS-ligated $CsPbBr_{0.5}I_{2.5}$ QDs deposed on the surface. High-density Pb is due to the dual contribution from both $CsPbBr_3$ PQDs and $MAPbI_3$ (scale bar = 3μm).

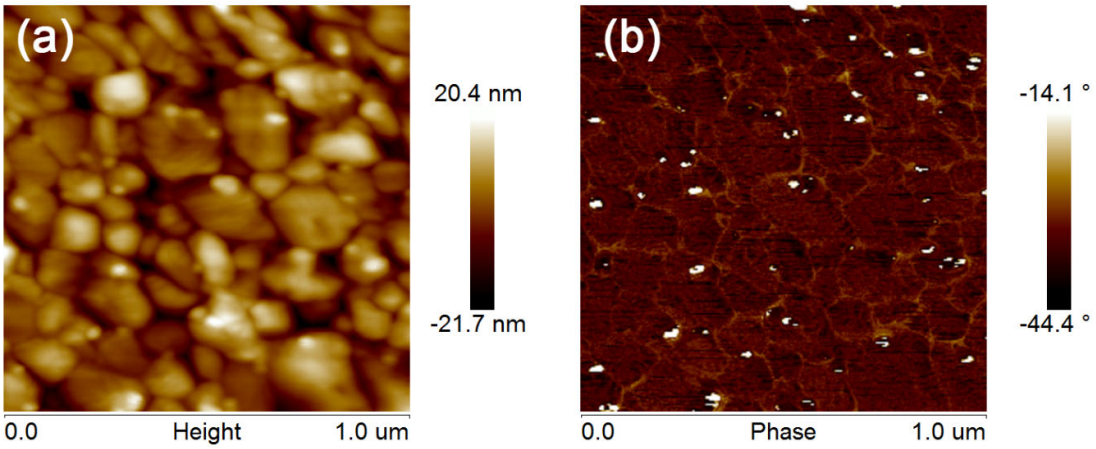

Figure S11. AFM (a) height and (b) phase images of perovskite $MAPbI_3$ film deposited with $CsPbBr_{0.5}I_{2.5}$ QDs.

Table S3. Photovoltaic parameters of pristine perovskite solar cell (PSC; control device) as well as PSCs incorporated with PS-ligated $CsPbBr_3$ QDs and $CsPbBr_{0.5}I_{2.5}$ QDs.

Devices	V_{OC} **(V)**	J_{SC} **(mA/cm^2)**	***FF*** **(%)**	***PCE*** **(%)**
Control	1.05	21.38	71.96	16.15
$CsPbBr_3$	1.10	19.17	56.58	11.93
$CsPbBr_{0.5}I_{2.5}$	1.07	23.20	72.51	18.00

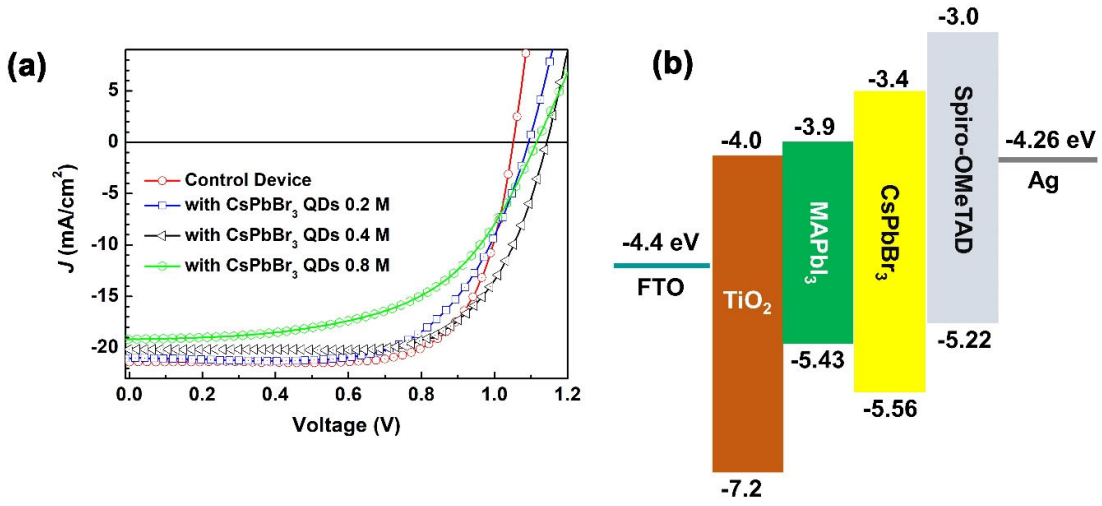

Figure S12. (a) *J-V* curves of perovskite solar cells without and with PS-ligated $CsPbBr_3$ QDs deposited at various concentrations. (b) Schematic illustration of energy levels of perovskite solar cells with $CsPbBr_3$ incorporated.

Table S4. Photovoltaic parameters of perovskite solar cells without and with the incorporation of $CsPbBr_3$ QDs of various concentrations at the $MAPbI_3$/Spiro-OMeTAD interface.

$CsPbBr_3$ QD (mol/L)	***V_{OC}* (V)**	***J_{SC}* (mA/cm^2)**	***FF* (%)**	***PCE* (%)**
0	1.05	21.38	71.96	16.15
0.2	1.09	21.00	64.48	14.76
0.4	1.15	20.16	68.50	15.88
0.8	1.10	19.17	56.58	11.93

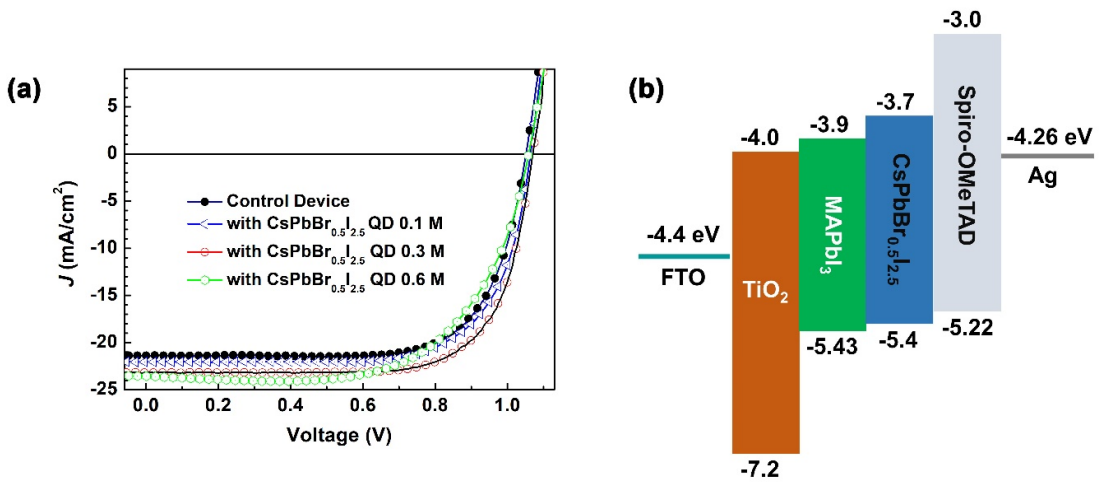

Figure S13. (a) *J-V* curves of perovskite solar cells before and after the deposition of $CsPbBr_{0.5}I_{2.5}$ quantum dots of various concentrations at the $MAPbI_3$/Spiro-OMeTAD interface. (b) Schematic illustration of energy levels of $CsPbBr_{0.5}I_{2.5}$ QDs-incorporated perovskite solar cells.

Table S5. Photovoltaic parameters of the perovskite solar cells without and with the incorporation of $CsPbBr_{0.5}I_{2.5}$ QDs of various concentrations at the $MAPbI_3$/Spiro-OMeTAD interface.

$CsPbBr_{0.5}I_{2.5}$ QD (mol/L)	***V_{OC}* (V)**	***J_{SC}* (mA/cm^2)**	***FF* (%)**	***PCE* (%)**
0	1.05	21.38	71.96	16.15
0.1	1.06	22.05	70.85	16.56
0.3	1.07	23.20	72.51	18.00
0.6	1.06	23.00	65.95	16.08

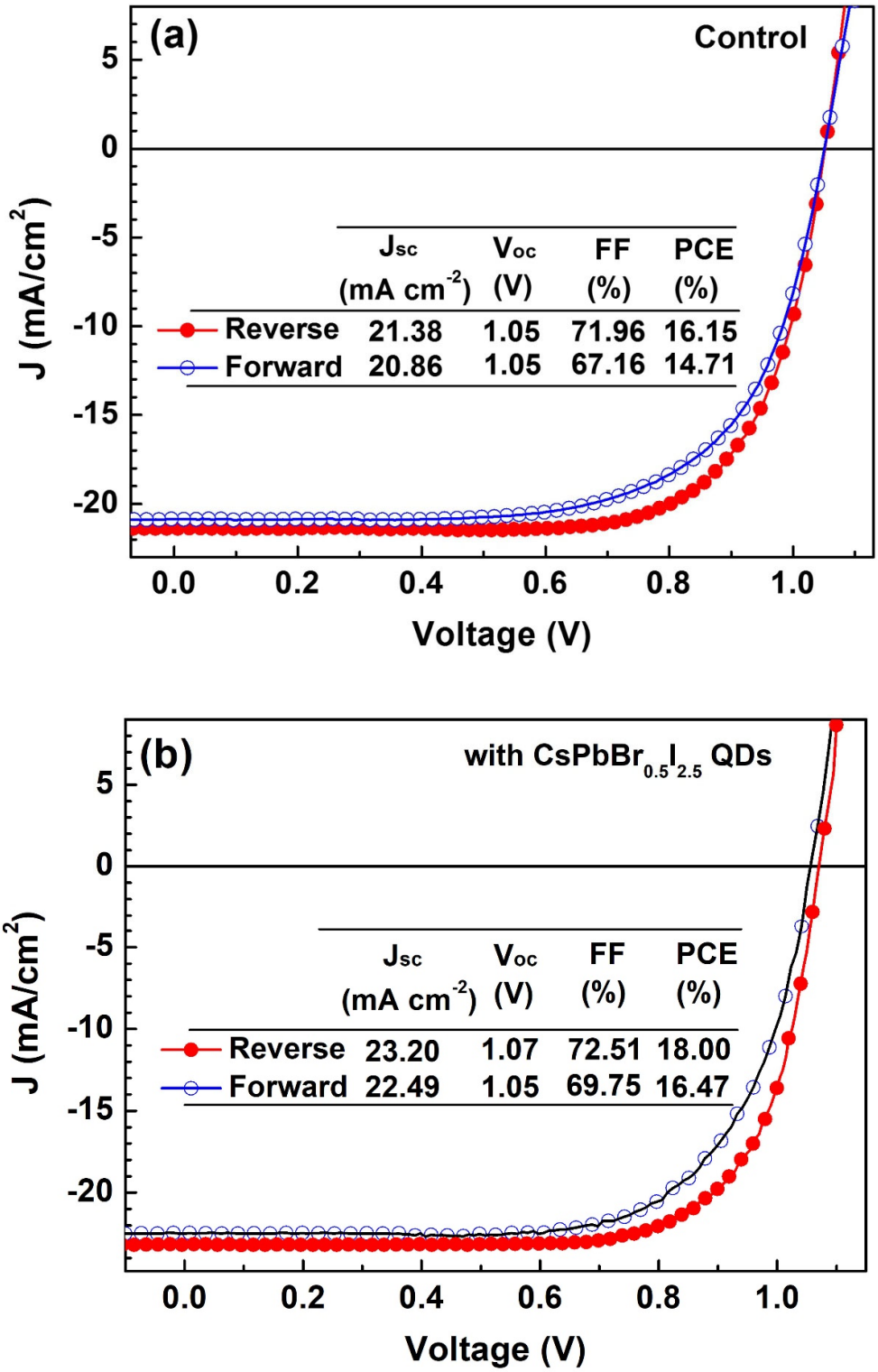

Figure S14. *J-V* characteristics for (a) control device and (b) $CsPbBr_{0.5}I_{2.5}$ QDs-incorporated device.

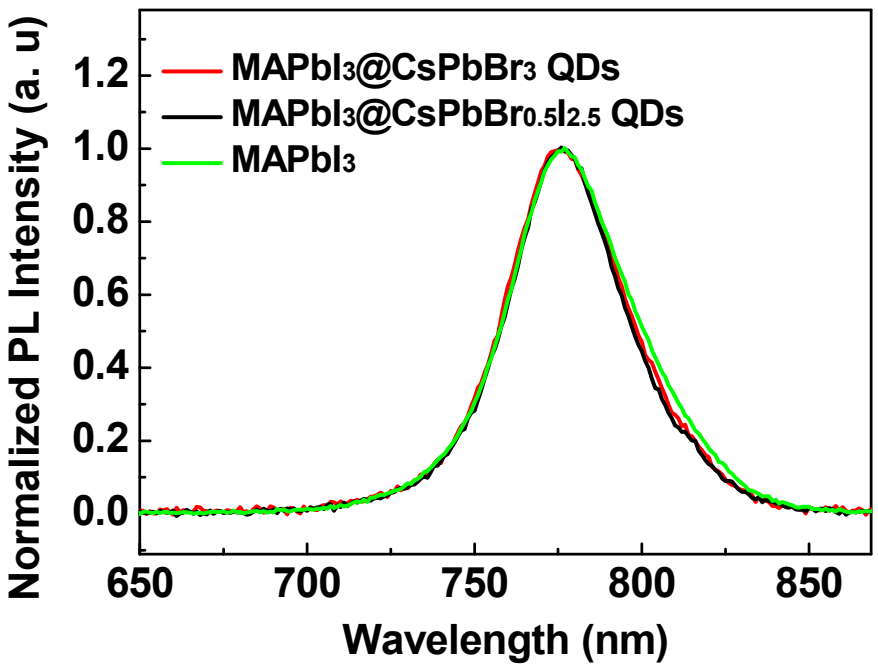

Figure S15. Normalized PL of perovskite films with and without PS-ligated $CsPbBr_xI_{3-x}$ QDs, respectively.

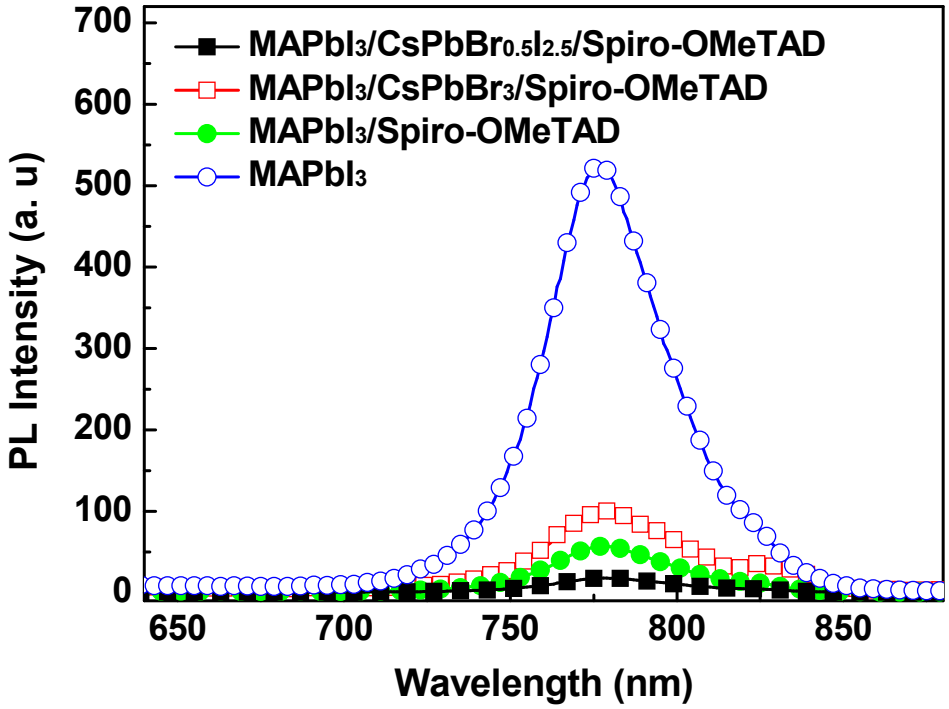

Figure S16. Steady-state photoluminescence spectra for pure $MAPbI_3$ film and $MAPbI_3$ film coated with Spiro-OMeTAD HTL as well as samples with PS-ligated $CsPbBr_3$ and $CsPbBr_{0.5}I_{2.5}$ QDs sandwiched between $MAPbI_3$ and Spiro-OMeTAD layers.

Table S6. Summary of PL decay parameters from a biexponential fitting of time-resolved PL decay curves for pristine $MAPbI_3$ and $MAPbI_3$/PS-ligated $CsPbBr_{0.5}I_{2.5}$ QDs, respectively.

Sample	A_1	τ_1 (ns)	A_2	τ_2 (ns)	τ_{ave} (ns)
$MAPbI_3$	0.680	17.76	0.206	102.59	71.74
$MAPbI_3$/ $CsPbBr_{0.5}I_{2.5}$	0.136	26.00	0.735	129.64	125.93

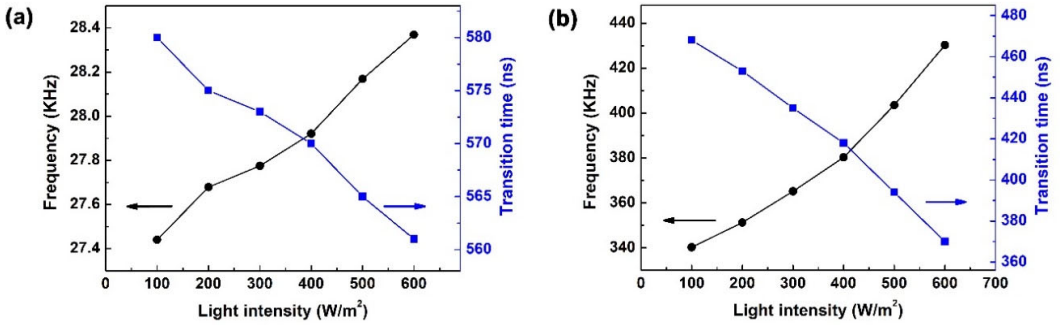

Figure S17. The intensity modulated photocurrent (IMPS) results of PSCs with and without the deposition of PS-ligated $CsPbBr_{0.5}I_{2.5}$ QDs at the $MAPbI_3$/Spiro-OMeTAD interface. Frequency and transition time (τ_d) as a function of incident light intensity for (a) control device, and (b) $CsPbBr_{0.5}I_{2.5}$ QDs-incorporated device.

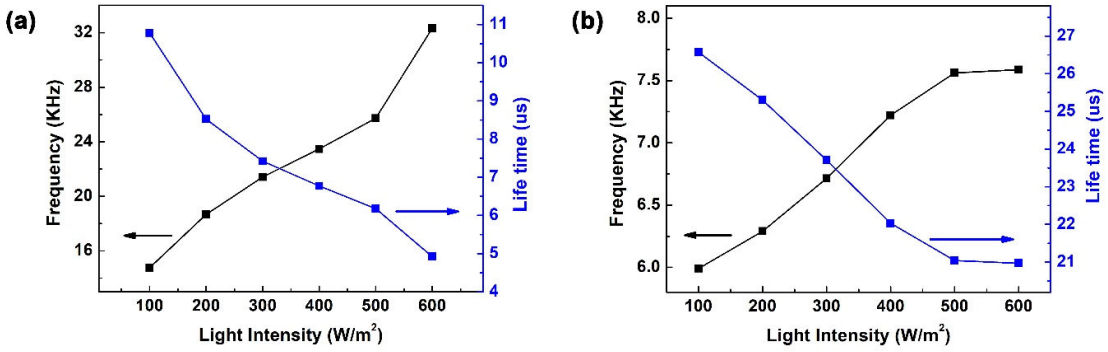

Figure S18. The intensity modulated photovoltage (IMVS) results of PSCs with and without the deposition of PS-ligated $CsPbBr_{0.5}I_{2.5}$ QDs at the $MAPbI_3$/Spiro-OMeTAD interface. Frequency and life time (τ_n) as a function of incident light intensity for (a) control device, and (b) $CsPbBr_{0.5}I_{2.5}$ QDs-incorporated device.

Table S7. Controlled intensity modulated photocurrent/photovoltage spectroscopy results of pristine PSCs (i.e., without PS-ligated $CsPbBr_{0.5}I_{2.5}$ QDs sandwiched at the $MAPbI_3$/Spiro-OMeTAD interface)

Light Intensity (W/m^2)	**Lifetime, τ_n (μs)**	**Transition time, τ_d (μs)**	η_{cc}
100	10.78	0.580	94.62%
200	8.52	0.575	93.25%
300	7.42	0.573	92.28%
400	6.77	0.570	91.58%
500	6.18	0.565	90.85%
600	4.92	0.561	88.60%

Table S8. Controlled intensity modulated photocurrent/photovoltage spectroscopy results of PSCs with PS-ligated $CsPbBr_{0.5}I_{2.5}$ QDs placed at the $MAPbI_3$/Spiro-OMeTAD interface.

Light Intensity (W/m^2)	**Lifetime, τ_n (μs)**	**Transition time, τ_d (μs)**	η_{cc}
100	26.57	0.468	98.24%
200	25.30	0.453	98.20%
300	23.71	0.435	98.16%
400	22.03	0.418	98.10%
500	21.04	0.394	98.12%
600	20.97	0.370	98.23%

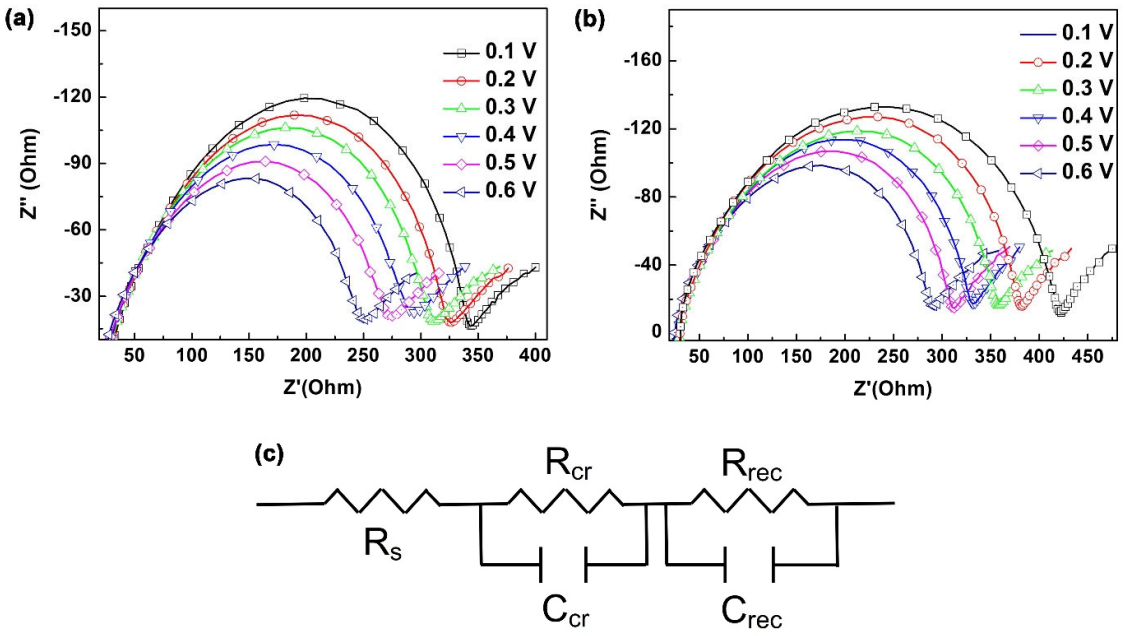

Figure S19. Nyquist plots of electrochemical impedance spectroscopy (EIS) measurements for (a) control device, (b) $CsPbBr_{0.25}I_{2.5}$ QDs-incorporated device under illumination at various applied bias from 0.1 to 0.6 V. (c) The equivalent circuit for fitting the impedance spectroscopy.

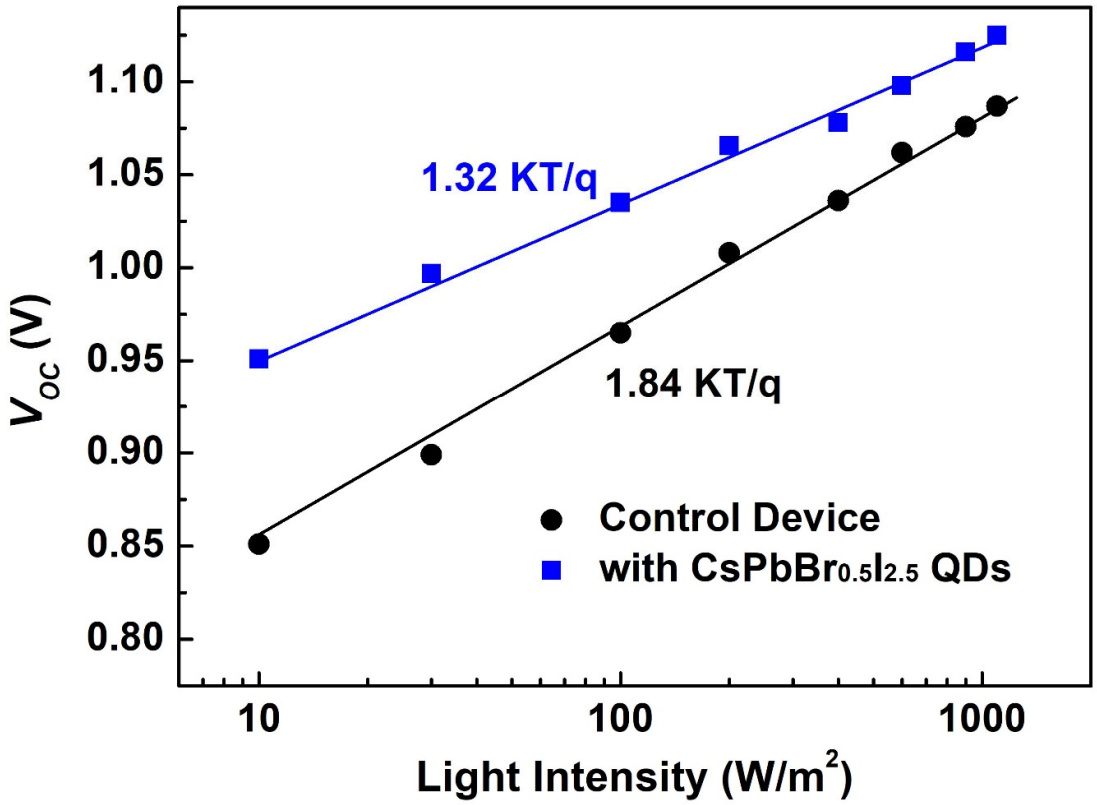

Figure S20. V_{OC} as a function of light intensity for both control and $CsPbBr_{0.25}I_{2.5}$ QDs-incorporated devices. The reduced ideality factor n is determined by the equation: $I = I_0 \exp(\frac{qV}{nk_BT})$, where k_B is the Boltzmann constant, T is absolute temperature, and q is elementary charge.

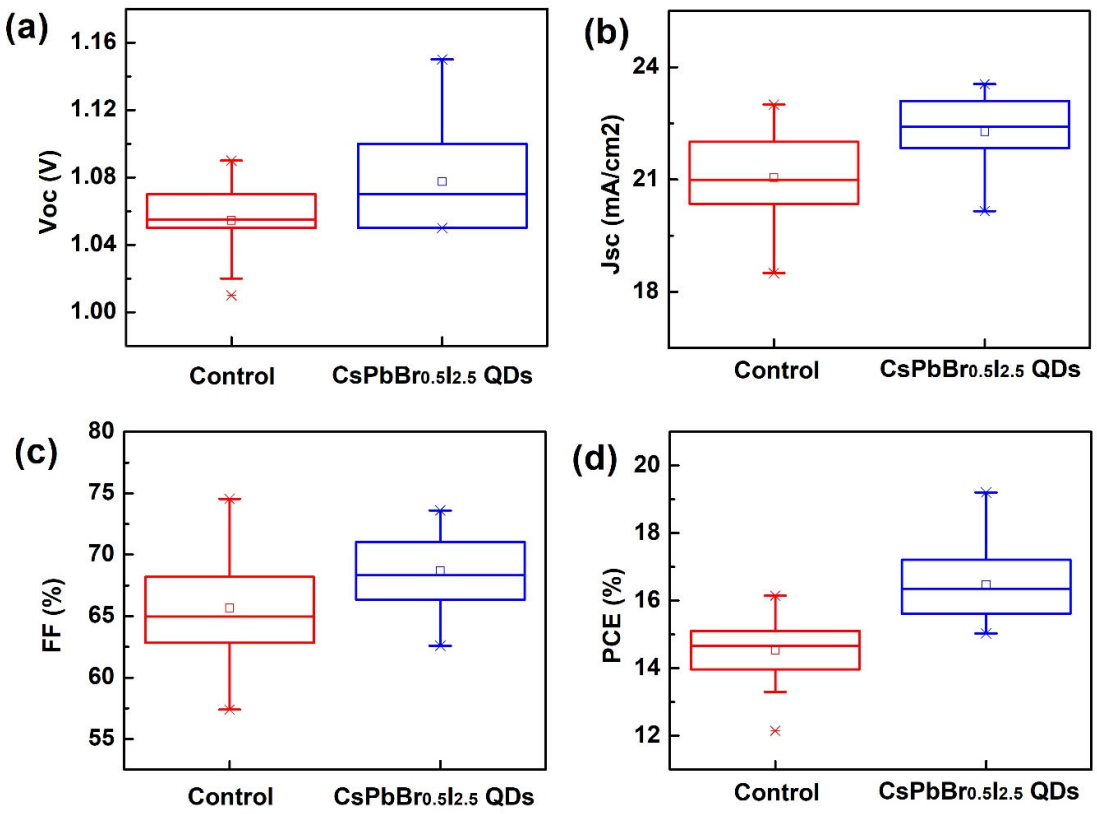

Figure S21. Device statistics of (a) V_{OC}, (b) J_{SC}, (c) fill factor, and (d) *PCE* of control and $CsPbBr_{0.25}I_{2.5}$ QDs-incorporated devices.

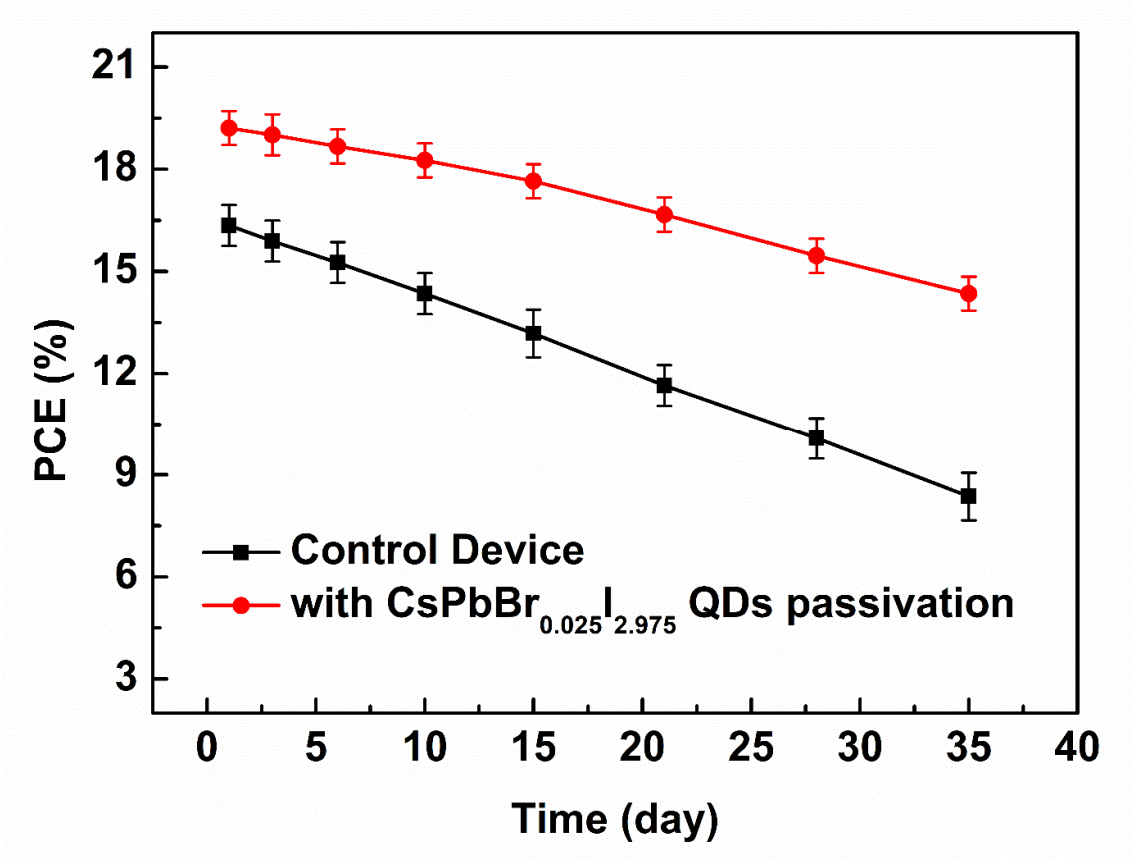

Figure S22. Stability of control and $CsPbBr_{0.025}I_{2.975}$ QDs-incorporated devices without encapsulation yet stored in a desiccator at room temperature (~25 ºC) with a relative humidity around 30%.

References

1. J. H. Heo, S. H. Im, J. H. Noh, T. N. Mandal, C.-S. Lim, J. A. Chang, Y. H. Lee, H.-j. Kim, A. Sarkar and M. K. Nazeeruddin, *Nat. Photonics*, 2013, **7**, 486.

2. X. Pang, L. Zhao, M. Akinc, J. K. Kim and Z. Lin, *Macromolecules,* 2011, **44**, 3746.

3. X. Pang, L. Zhao, C. Feng and Z. Lin, *Macromolecules* 2011, **44**, 7176.